

nickelate 초전도체의 대안 연구.

height of apical oxygen of $d_{x^2-y^2}$ & $d_{3z^2-r^2}$ 의 차이가 바뀌었다.

low spin issue는 고려되었지 않다.

Designing nickelate superconductors with d^8 configuration exploiting mixed-anion strategy

Naoya Kitamine,¹ Masayuki Ochi,¹ and Kazuhiko Kuroki¹

¹Department of Physics, Osaka University, 1-1 Machikaneyama-cho, Toyonaka, Osaka, 560-0043, Japan

(Dated: July 3, 2020)

Inspired by a recently proposed superconducting mechanism for a new cuprate superconductor $\text{Ba}_2\text{CuO}_{3+\delta}$, we theoretically design an unconventional nickelate superconductor with d^8 electron configuration. Our strategy is to enlarge the on-site energy difference between $3d_{x^2-y^2}$ and other $3d$ orbitals by adopting halogens or hydrogen as out-of-plane anions, so that the $3d$ bands other than $d_{x^2-y^2}$ lie just below the Fermi level for the d^8 configuration, acting as incipient bands that enhance superconductivity. We also discuss a possible relevance of the present proposal to the recently discovered superconductor $(\text{Nd}, \text{Sr})\text{NiO}_2$.

The two families of high T_c superconductors, cuprates[1] and iron based compounds[2], have often been contrasted as single-orbital vs. multiorbital systems. Namely, in the cuprates, only the $d_{x^2-y^2}$ orbital plays the main role while in the iron-based superconductors, d_{xy} , d_{xz} and d_{yz} orbitals largely contribute to the electronic structure around the Fermi level. Recently, however, there has occurred a possible paradigm shift to this picture, owing to some new experimental findings. One of such experiments is the discovery of high T_c superconductivity in $\text{Ba}_2\text{CuO}_{3+\delta}$ [3], where the height of the apical oxygen is so low that the energy levels of $d_{x^2-y^2}$ and $d_{3z^2-r^2}$ can be reversed compared to conventional cuprates. Another example is a highly overdoped CuO_2 monolayer grown on $\text{Bi}_2\text{Sr}_2\text{CaCu}_2\text{O}_{8+\delta}$ [4], where the Fermi level is significantly lowered so that it may reach the $d_{3z^2-r^2}$ band [5].

For $\text{Ba}_2\text{CuO}_{3+\delta}$, various theoretical studies have been performed[6–12], many of which treat multiorbital models. In Ref.[12], two of the present authors have introduced a two-orbital model consisting of Wannier orbitals with $d_{x^2-y^2}$ and $d_{3z^2-r^2}$ symmetries, where s -wave superconductivity with reversed gap sign between the two bands ($s\pm$ -wave pairing) is found to be strongly enhanced near half-filling when the energy level offset ΔE between $d_{3z^2-r^2}$ and $d_{x^2-y^2}$ orbitals is enlarged so that the bottom of the $d_{3z^2-r^2}$ band is positioned just above the Fermi level. The strong enhancement of superconductivity was explained by transforming the two-orbital model to the bilayer Hubbard model, where the two orbitals of the former model correspond to the bonding and antibonding orbitals of the latter, and hence the orbital level offset ΔE in the former transforms to $2t_\perp$ in the latter with t_\perp being the vertical hopping between the layers in the bilayer model. The bilayer Hubbard model has been intensively studied from the past[13–29], and $s\pm$ -wave superconductivity is found to be strongly enhanced near half-filling when t_\perp is several times larger than the in-plane hopping and the Fermi level lies in the vicinity of one of the bands[13, 18, 23–28]. Nowadays, a band sitting just below (or above) the Fermi level is often re-

ferrered to as an incipient band, and has attracted interest in the study of iron-based superconductors[30–37], bilayer and ladder-type lattices[26–29, 38–42], and flat band superconductivity[43–46]. The two-orbital to bilayer transformation is mathematically exact when there is no hybridization between the two orbitals and also $U = U' = J = J'$ is satisfied, where U , U' , J , and J' are the intra-orbital repulsion, inter-orbital repulsion, Hund's coupling, and the pair hopping interaction, respectively[12, 47]. In reality, $U > U' > J, J'$ and the inter-orbital hybridization is present, but the analogy between the two models turns out to be approximately valid even in the realistic situation[12].

Actually, a situation where the Fermi level lies close to the $d_{3z^2-r^2}$ band edge is realized in a cuprate $(\text{La}, \text{Sr})_2\text{CuO}_4$. One of the present authors and his colleagues have pointed out that the presence of the $d_{3z^2-r^2}$ band around the Fermi level is the origin of the suppression of T_c of the d -wave superconductivity in this material[48–51] due to the orbital component mixture around the antinodal regime. The difference between $(\text{La}, \text{Sr})_2\text{CuO}_4$ and $\text{Ba}_2\text{CuO}_{3+\delta}$ in Ref.[12] is that in the former, the e_g bands are close to 3/4-filling on average (nearly two electrons in $d_{3z^2-r^2}$ and one electron in $d_{x^2-y^2}$), while the latter is closer to half-filling.

The above consideration brings us to an idea of realizing incipient-band-enhanced superconductivity in nickelates, where the e_g bands become half-filled on average for the natural Ni^{2+} valence, namely, the d^8 electron configuration. Actually, if all the bands other than $d_{x^2-y^2}$ sink below the Fermi level for the d^8 configuration, a pair of $d_{x^2-y^2}$ and any other d orbital is half-filled (two electrons per two orbital on average), so if small amount of electrons are doped into such systems, we may expect enhanced $s\pm$ -wave superconductivity. To enlarge the energy level offset between $d_{x^2-y^2}$ and $d_{3z^2-r^2}$ orbitals, we adopt a mixed-anion strategy[52], namely, we chose halogens or hydrogens instead of oxygens as out-of-plane anions (which corresponds to enhancing t_\perp in the bilayer system), for which we end up with the composition of $AE_2\text{NiO}_2X_2$ ($AE=\text{Ca}, \text{Sr}$, $X=\text{H}, \text{F}, \text{Cl}, \text{Br}, \text{I}$).

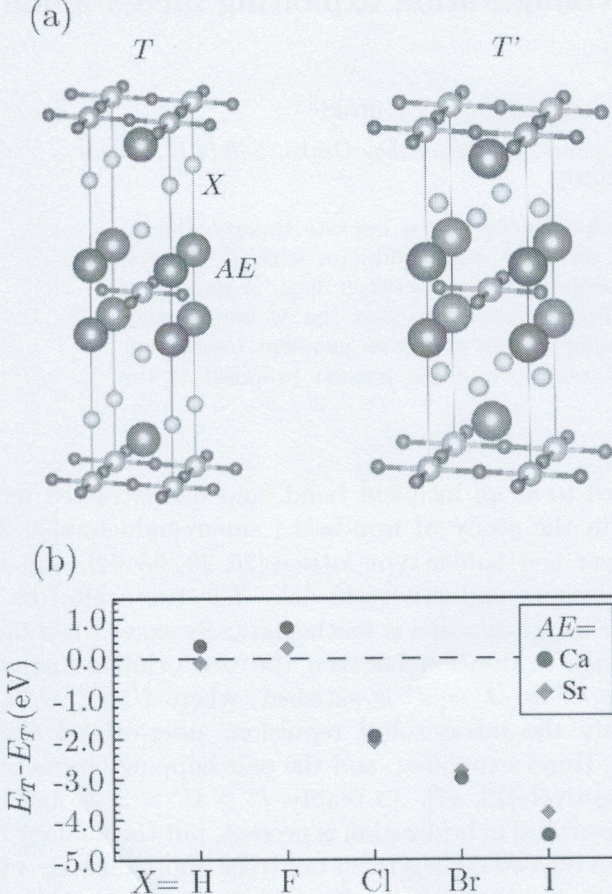


FIG. 1. (a) *T* and *T'* crystal structures. (b) The total energy difference per formula unit between *T* and *T'* structures for various choices of elements.

We note that similar materials have been proposed in Ref.[53] in the context of a recently discovered superconductor (Nd,Sr)NiO₂[54], but there, the aim was to construct ideal single band systems with d^9 electron configuration, where bands other than Ni $d_{x^2-y^2}$ do not intersect the Fermi level for the mother compound. In fact, in the present study, we conversely discuss a possible relevance of the present d^8 proposal to the superconductivity of (Nd,Sr)NiO₂.

We consider *T*(K₂NiO₄) and *T'* (Fig.1) structures as candidates for possible crystal structures[55]. We also take La₂NiO₄ (*T* structure) as a reference system with d^8 configuration. We perform structural optimization using the PBE-GGA exchange-correlation functional[56] and the projector augmented wave method[57]. For this purpose, we use Vienna ab initio Simulation Package (VASP)[58–61]. $12 \times 12 \times 12 k$ mesh and a plane-wave cut-off energy of 550 eV was used. After the structural optimization, we perform first-principles band-structure calculation using WIEN2k code[62]. We adopt RKmax=7 (6 for oxy-hydrides), and take $12 \times 12 \times 12 k$ mesh in the self-consistent-field calculations. From the calculated band structures, we extract the Wannier functions[63, 64]

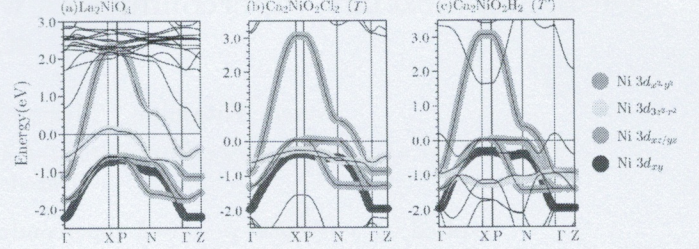


FIG. 2. The band structures of (a) La₂NiO₄, (b) Ca₂NiO₂Cl₂ (*T*), (c) Ca₂NiO₂H₂ (*T'*). The band dispersion of the five orbital model is superposed to the first principles bands.

of five Ni 3d orbitals using the Wien2Wannier[65] and Wannier90[66] codes. Throughout the study, the spin-orbit coupling is neglected.

In Fig.1(b), we plot the total energy difference between the two structures for all choices of AE and X elements. It is found that for $X=\text{Cl}, \text{Br}$ and I , the *T* structure has lower energy ($E_T - E_{T'} < 0$), while the difference between the two is small for $X=\text{H}, \text{F}$. In fact, phonon calculation of Ba_{0.5}La_{0.5}NiO₂F₂ in Ref.[53] shows appearance of imaginary modes for the *T* structure, but not for *T'*, which suggests stability of the latter. The optimized lattice constants presented in the supplemental material exhibit a trend where the in-plane lattice constant a becomes larger as the ion radius of element X or AE is increased.

The first principles band structures obtained for the optimized lattice structures of La₂NiO₄ (*T*), Ca₂NiO₂Cl₂ (*T*), and Ca₂NiO₂H₂ (*T'*) are shown in Fig.2. The energy dispersion of the five orbital model is superposed to the first principles bands for each material. The band structures of materials with other elements are presented in the supplemental material. It can be noticed that in the mixed-anion materials, $d_{3z^2-r^2}$ band totally sinks below the Fermi level (E_F) despite the d^8 electron configuration with the $d_{x^2-y^2}$ band partially filled, in sharp contrast to the case of La₂NiO₄. The entire d_{xy} band also lies below E_F , while the top of $d_{xz/yz}$ bands intersects E_F .

In Fig.3, we plot the on-site energy (ΔE) of the d orbitals with respect to that of $d_{x^2-y^2}$ in the five orbital model. Let us focus on the crystal structure having the lower total energy (denoted by the solid symbols). $|\Delta E|$ tends to be larger (i.e., the energy level is lowered since $\Delta E < 0$) as the ion radius of X is reduced within $X=\text{Cl}, \text{Br}$ and I . This is due to the smaller in-plane lattice constant (shorter Ni-O distance), which pushes up the $d_{x^2-y^2}$ energy level. For the *T'* structure, the on-site energy of the $d_{3z^2-r^2}$ orbital is strongly reduced due to the absence of the apical anions, but the t_{2g} orbitals are pushed up compared to those in the *T* structure. If we compare $AE=\text{Ca}$ and Sr , $|\Delta E|$ of the t_{2g} orbitals are reduced in the former compared to the latter, while that of $d_{3z^2-r^2}$ is less affected. This is because the lattice constants a and c are shorter for $AE=\text{Ca}$ than for Sr .

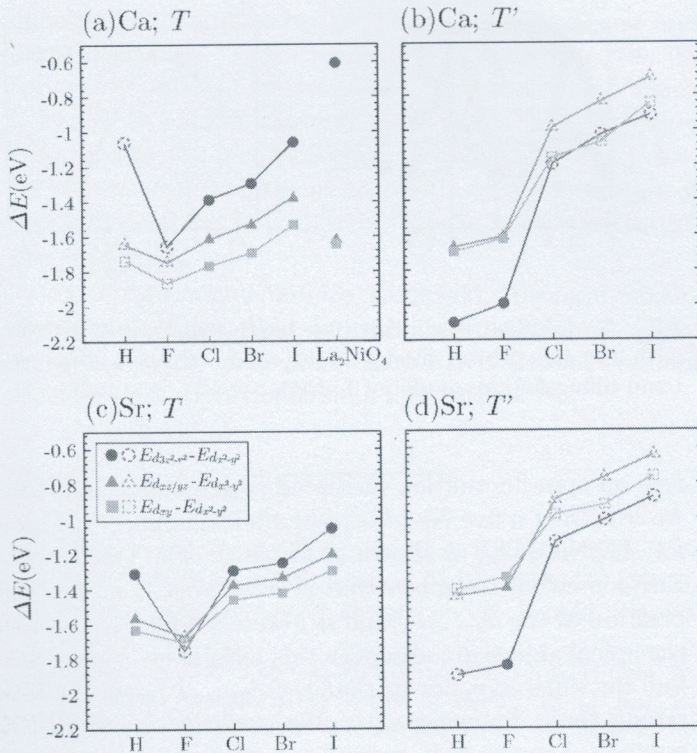


FIG. 3. The on-site energy of the d orbitals other than the $d_{x^2-y^2}$ orbital, measured from that of $d_{x^2-y^2}$. (a) $AE=Ca$; T , (b) Ca ; T' , (c) Sr ; T , (d) Sr ; T' . Here the solid (dashed) symbols denote the lattice structure with lower (higher) total energy. As a reference, the values of ΔE for La_2NiO_4 are plotted in (a).

We now analyze superconductivity based on the obtained five-orbital models. We assume on-site intra- and inter-orbital interactions, U , U' , J and J' , and the many-body study of this model is performed within the fluctuation exchange approximation (FLEX)[67]. We mainly adopt $U = 4\text{eV}$, $J = J' = U/10$, $U' = U - 2J$, but also discuss the interaction dependence in the supplemental material. A relatively large U is taken in accord with a study for $LaNiO_2$ [70]. We obtain the renormalized Green's function by solving the Dyson's equation in a self-consistent calculation. The obtained Green's function and the pairing interaction mediated mainly by spin-fluctuations are plugged into the linearized Eliashberg equation. Since the eigenvalue λ of the equation reaches unity at $T = T_c$, here we adopt λ , obtained at a fixed temperature of $T = 0.01\text{eV}$, to measure how close the system is to superconductivity. The eigenfunction of the Eliashberg equation will be called the gap function. In the FLEX calculation, $16 \times 16 \times 4$ (k_x, k_y, k_z) mesh and 2048 Matsubara frequencies were taken.

In Fig.4(a)(b), we plot the eigenvalue of the Eliashberg equation against the band filling, varied assuming rigid band, for various materials with the crystal structure (T or T') having lower total energy. In all mixed-anion compounds, λ is peaked at around $n = 4.1$ to 4.2 ,

which corresponds to 10 to 20% electron doping starting from the stoichiometric band filling of $n = 4$. The compounds having the largest maximum λ are $Ca_2NiO_2Cl_2$ and $Ca_2NiO_2H_2$. These maximum values of λ are much larger compared to that of La_2NiO_4 [72], and they are in fact even larger than that of $HgBa_2CuO_4$, a $T_c = 100\text{K}$ superconductor, obtained in the same manner[70].

The gap function presented in Fig.4(c) for the case of $Ca_2NiO_2Cl_2$ with $n = 4.125$ shows that the four bands other than $d_{x^2-y^2}$ have the same sign of the gap, opposite to that of the $d_{x^2-y^2}$ band (see the supplemental material for the countour plot of the gap). In this sense, this is $s\pm$ -wave pairing with the four bands other than $d_{x^2-y^2}$ being incipient, namely, located below the Fermi level, with the $d_{xz/yz}$ band top being the closest to the Fermi level. In order to see the role played by each orbital in more detail, we extract one, two, three, or four orbitals from the five orbital model, and apply FLEX to those multiorbital models to obtain λ in a similar manner. From Fig.4(d), it can be seen that λ in the $d_{x^2-y^2} + d_{xz/yz}$ model is strongly enhanced compared to the single orbital model consisting only of $d_{x^2-y^2}$, indicating the important role played by the incipient $d_{xz/yz}$ bands. On the other hand, adding d_{xy} and/or $d_{3z^2-r^2}$ orbitals to the $d_{x^2-y^2} + d_{xz/yz}$ model does not strongly affect λ . Our interpretation is that the interaction between d_{xy} (or $d_{3z^2-r^2}$) and $d_{x^2-y^2}$ orbitals enhances superconductivity because the signs of

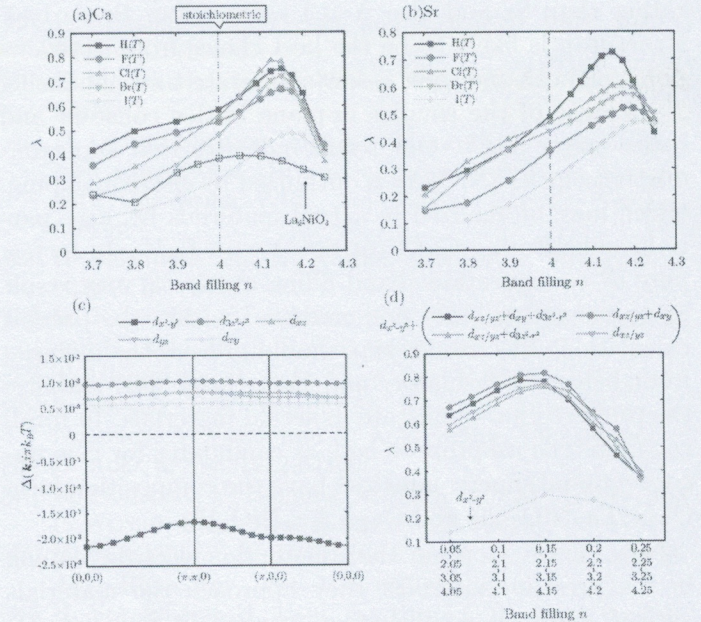


FIG. 4. Eigenvalue of the Eliashberg equation λ at $T = 0.01\text{eV}$ against the band filling for (a) $AE=Ca$ and (b) Sr . In (a), also the results for La_2NiO_4 are plotted as a reference. (c) Gap function of $Ca_2NiO_2Cl_2$ for $n = 4.125$ in the orbital representation. (d) Similar plot of λ obtained for various two, three, and four orbital models (see text) of $Ca_2NiO_2Cl_2$. The horizontal axis is the band filling (for the single orbital to the five orbital model from top to bottom).

the gap are opposite, but the interaction between d_{xy} (or $d_{3z^2-r^2}$) and d_{xz}/yz gives negative contribution to superconductivity because of the same sign of the gap. Since λ is dominated by the position of the d_{xz}/yz bands, the materials having larger energy difference between $d_{x^2-y^2}$ and d_{xz}/yz orbitals, corresponding to larger t_\perp in the bilayer Hubbard model[12], tend to exhibit larger λ . On the other hand, it should be stressed that the strong reduction of λ for La_2NiO_4 compared to mixed-anion materials mainly comes from the the small $|\Delta E|$ for the $d_{3z^2-r^2}$ orbital; the $d_{3z^2-r^2}$ band intersecting the Fermi level gives rise to strong development of low energy spin fluctuations, which works destructively against superconductivity, as in the case of the bilayer Hubbard model with small t_\perp [24, 25, 27, 28]. Further analysis on the role played by each orbital is given in the supplemental material.

We note that all of our calculations assume low-spin state, while nickelates with d^8 configuration can take high-spin states when the d -level splittings are small. In fact, the reference system in our study La_2NiO_4 is actually well known to be in the high-spin state, and also $\text{Sr}_2\text{NiO}_2\text{Cl}_2$, synthesized in Ref.[68], was found to be in a high-spin state. On the other hand, a hypothetical infinite layer nickelate SrNiO_2 , without apical anions, was theoretically shown to have a low-spin ground state[69]. Hence, large $|\Delta E|$ is not only preferable for enhancing T_c , but it is also favorable from the viewpoint of realizing a low-spin ground state. In this sense, $AE=\text{Ca}$ rather than Sr and also $X=\text{Cl}$ rather than Br or I (T structure), is likely to be the best choice from the viewpoint of both realizing a low-spin state and enhancing T_c because of the smaller in-plane lattice constant and hence larger $|\Delta E|$. Our result indicates that superconductivity in $AE_2\text{NiO}_2X_2$ is optimized by electron doping, which may be realized in actual materials by, e.g., partially substituting Ca^{2+} (or Sr^{2+}) with La^{3+} . In fact, a pure d^8 configuration (band filling of $n = 4$) may result in an insulating state not predicted within the present calculation. Electron doping should prevent the material from being an insulator, and hence may also stabilize the preferred low-spin state in actual materials. In total, the materials we propose here as candidates for new unconventional superconductors have the composition form $\text{Ca}_{2-x}\text{La}_x\text{NiO}_2\text{Cl}_2$ and $\text{Ca}_{2-x}\text{La}_x\text{NiO}_2\text{H}_2$.

Now, if we increase the amount of electron doping in the present materials, they approach the materials with d^9 electron configuration studied in Refs.[53, 71] in the context of a recently discovered superconductor $(\text{Nd},\text{Sr})\text{NiO}_2$ [54]. Then, conversely, it is interesting to see how the d^9 and d^8 states are connected in $(\text{Nd},\text{Sr})\text{NiO}_2$ by hypothetically removing the electrons. Here we consider LaNiO_2 adopting the experimentally determined lattice parameters of NdNiO_2 to avoid the ambiguity regarding the treatment of the f electrons in Nd [70]. Since a previous study has shown that the La 5d orbitals have small ef-

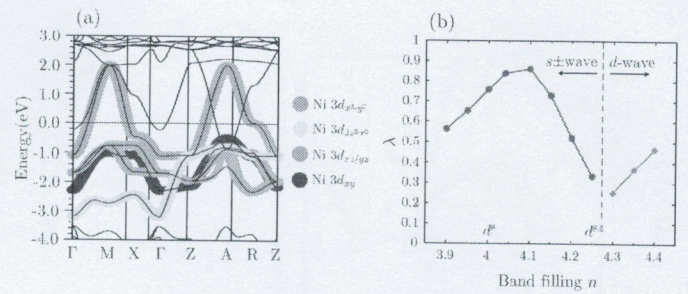


FIG. 5. (a) The first principles band structure of LaNiO_2 with the five-orbital model superposed. (b) λ against the band filling for the model of LaNiO_2 .

fect on spin-fluctuation-mediated superconductivity[70], we construct a five Ni-3d-orbital model similarly to those for $AE_2\text{NiO}_2\text{Cl}_2$, as shown in Fig.5(a). The band structure somewhat resembles that of $AE_2\text{NiO}_2\text{Cl}_2$ in that the position of the $d_{3z^2-r^2}$ band is lowered, which is because the apical anions are absent in this infinite layer material, but the difference lies in that the $d_{3z^2-r^2}$ band exhibits strong three dimensionality. We perform similar FLEX analysis of superconductivity for this model by hypothetically varying the band filling assuming a rigid band. As expected from our results on $AE_2\text{NiO}_2X_2$, there appears a peak in λ close to $n = 4$, i.e., the d^8 configuration, in addition to the already known d -wave superconductivity around $n = 4.5$, the d^9 configuration.

Although we believe that the mechanism similar to the cuprates, where only the $d_{x^2-y^2}$ band plays an important role, is a strong candidate for the superconducting mechanism of $(\text{Nd},\text{Sr})\text{NiO}_2$ [70, 73–75], the present analysis suggests that their might be an alternative scenario where Ni 3d orbitals other than $d_{x^2-y^2}$ play the role of incipient bands. In fact, as studied in Ref.[76], $(\text{Nd},\text{Sr})\text{NiO}_2\text{H}$ may form during the reduction process by CaH_2 , which would reduce the number of d electrons[77]. It will then be an interesting future problem to carefully examine the Ni valence in $(\text{Nd},\text{Sr})\text{NiO}_2$. Also, the gap function would be of interest since d -wave should be realized for the d^9 pairing mechanism, whereas s -wave is expected for the d^8 scenario. In fact, while finalizing the present paper, a tunneling spectroscopy experiment has been reported[78], where s -wave and d -wave-like gaps have been observed, depending on the position on the sample. The experiment has been interpreted in terms of the gap with different symmetry opening on different Fermi surfaces, which was suggested theoretically[79]. From our viewpoint, the position dependence of the pairing symmetry might originate from the inhomogeneity of the residual hydrogen during the reduction process[80].

To conclude, we have designed an unconventional nickelate superconductor with nearly d^8 electron configuration, where superconductivity is enhanced by the bands other than $d_{x^2-y^2}$ playing a role of the incipient bands. The key idea is to exploit the mixed-anion strategy to

high
to
low
spin

enlarge the on-site energy difference between $d_{x^2-y^2}$ and other d orbitals. This corresponds to increasing the interlayer hopping t_\perp of the bilayer Hubbard model, which is known to exhibit $s\pm$ -wave superconductivity strongly enhanced by the incipient band effect for large t_\perp . Possible relevance of the present proposal to the observation of superconductivity in (Nd,Sr)NiO₂ is an interesting future problem.

We acknowledge Kimihiko Yamazaki, Hirofumi Sakakibara, and Hideo Aoki for valuable discussions. This study is supported by JSPS KAKENHI Grant Numbers JP18H01860, JP19H04697, and JP19H05058.

-
- [1] For a review, see e.g. B. Keimer, S.A. Kivelson, M.R. Norman, S. Uchida, and J. Zaanen, *Nature* **518**, 179 (2015).
[2] For a review, see e.g., H. Hosono and K. Kuroki, *Physica C* **514**, 399 (2015).
[3] W. M. Li, J. F. Zhao, L. P. Cao, Z. Hu, Q. Z. Huang, X. C. Wang, Y. Liu, G. Q. Zhao, J. Zhang, Q. Q. Liu, R. Z. Yu, Y. W. Long, H. Wu, H. J. Lin, C. T. Chen, Z. Li, Z. Z. Gong, Z. Guguchia, J. S. Kim, G. R. Stewart, Y. J. Uemura, S. Uchida, and C. Q. Jin, *Proc. Natl. Acad. Sci. U.S.A.* **116**, 12156 (2019).
[4] Y. Zhong, Y. Wang, S. Han, Y. Lv, W. Wang, D. Zhang, H. Ding, Y. Zhang, L. Wang, K. He, R. Zhong, J.A. Schneeloch, G. Gu, C. Song, X. Ma, and Q.K. Xue, *Sci. Bull.* **61**, 1239 (2016).
[5] K. Jiang, X. Wu, J. Hu, and Z. Wang, *Phys. Rev. Lett.* **121**, 227002 (2018).
[6] T. Maier, T. Berlijn, and D. J. Scalapino, *Phys. Rev. B* **99**, 224515 (2019).
[7] K. Liu, Z. Y. Lu, and T. Xiang, *Phys. Rev. Materials*, **3**, 044802 (2019).
[8] C. Le, K. Jiang, Y. Li, S. Qin, Z. Wang, F. Zhang, and J. Hu, arXiv:1909.12620 (2019).
[9] Y. Li, S. Du, Z.-Y. Weng, and Z. Liu, arXiv:1909.08304 (2019).
[10] Y. Ni, Y.-M. Quan, J. Liu, Y. Song, and L.-J. Zou, arXiv:1912.10580 (2019).
[11] Z. Wang, S. Zhou, W. Chen, and F.-C. Zhang, arXiv:1912.12581 (2019).
[12] K. Yamazaki, M. Ochi, D. Ogura, K. Kuroki, H. Eisaki, S. Uchida, and H. Aoki, arXiv:2003.04015.
[13] N. Bulut, D. J. Scalapino, and R. T. Scalettar, *Phys. Rev. B* **45**, 5577 (1992).
[14] R. T. Scalettar J.W. Cannon, D. J. Scalapino, and R. L. Sugar, *Phys. Rev. B* **50**, 13419 (1994).
[15] R. E. Hetzel, W. von der Linden, and W. Hanke, *Phys. Rev. B* **50**, 4159 (1994).
[16] R. R. dos Santos, *Phys. Rev. B* **51**, 15540 (1995).
[17] A.I. Liechtenstein, I.I. Mazin, and O.K. Andersen, *Phys. Rev. Lett.* **74**, 2303 (1995).
[18] K. Kuroki, T. Kimura, and R. Arita, *Phys. Rev. B* **66**, 184508 (2002).
[19] S. S. Kancharla and S. Okamoto, *Phys. Rev. B* **75**, 193103 (2007).
[20] K. Bouadim G. G. Batrouni, F. Hebert, and R. T. Scalettar, *Phys. Rev. B* **77**, 144527 (2008).
[21] N. Lanata, P. Barone, and M. Fabrizio, *Phys. Rev. B* **80**,

- 224524 (2009).
[22] H. Zhai, F. Wang, and D.-H. Lee, *Phys. Rev. B* **80**, 064517 (2009).
[23] T. Maier and D.J. Scalapino, *Phys. Rev. B* **84**, 180513(R) (2011).
[24] V. Mishra, D.J. Scalapino, and T. Maier, *Sci. Rep.* **6**, 32078 (2016).
[25] M. Nakata, D. Ogura, H. Usui, and K. Kuroki, *Phys. Rev. B* **95**, 214509 (2017).
[26] T.A. Maier, V. Mishra, G. Balduzzi, and D.J. Scalapino, *Phys. Rev. B* **99**, 140504(R) (2019).
[27] K. Matsumoto, D. Ogura and K. Kuroki, *J. Phys. Soc. Jpn.* **89**, 044709 (2020).
[28] D. Kato and K. Kuroki, *Phys. Rev. Research*, **2**, 023156 (2020).
[29] M. Kainth and M.W. Long, arXiv:1904.07138.
[30] A. Charnukha, D.V.Evtushinsky, C.E. Matt, N. Xu, M. Shi, B.Büchner, N.D. Zhigadlo, B. Batlogg, and V. Borisenko, *Sci. Rep.* **5**, 18273 (2015).
[31] H. Miao, T. Qian, X. Shi, P. Richard, T.K.Kim, M. Hoesch, L.Y.Xing, X.-C. Wang, C.-Q.Jin, J.-P. Hu, and H. Ding, *Nat. Commun.* **6**, 6056 (2015).
[32] F. Wang, F. Yang, M. Gao, Z.-Y. Lu, T. Xiang, and D.-H. Lee, *Europhys. Lett.* **93**, 57003 (2011).
[33] Y. Bang, *New J. Phys.* **16**, 023029 (2014).
[34] X. Chen, S. Maiti, A. Linscheid, and P. J. Hirschfeld, *Phys. Rev. B* **92**, 224514 (2015).
[35] P.J. Hirschfeld, M.M. Korshunov and I.I. Mazin, *Rep. Prog. Phys.* **74**, 124508 (2011).
[36] Y. Bang, *New J. Phys.* **18**, 113054 (2016).
[37] Y. Bang, *Sci. Reports* **9**, 3907 (2019).
[38] K. Kuroki, T. Higashida, R. Arita, *Phys. Rev. B* **72**, 212509 (2005).
[39] K. Matsumoto, D. Ogura, and K. Kuroki, *Phys. Rev. B* **97**, 014516(2018).
[40] D. Ogura, H. Aoki, K. Kuroki, *Phys. Rev. B* **96**, 184513 (2017).
[41] D. Ogura, Springer Theses, "Theoretical Study of Electron Correlation Driven Superconductivity in Systems with Coexisting Wide and Narrow Bands", Springer (2019).
[42] H. Sakamoto and K. Kuroki, *Phys. Rev. Research*, **2**, 022055(R) (2020).
[43] K. Kobayashi, M. Okumura, S. Yamada, M. Machida, and H. Aoki, *Phys. Rev. B* **94**, 214501 (2016).
[44] T. Misumi and H. Aoki, *Phys. Rev. B* **96**, 155137 (2017).
[45] S. Sayyad, E.W. Huang, M. Kitatani, M.-S. Vaezi, Z. Nussinov, A. Vaezi, and H. Aoki, arXiv: 1903.09888.
[46] H. Aoki, arXiv: 1912.04469.
[47] H. Shinaoka, Y. Nomura, S. Biermann, M. Troyer, and P. Werner, *Phys. Rev. B* **92**, 195126 (2015).
[48] H. Sakakibara, H. Usui, K. Kuroki, R. Arita, and H. Aoki, *Phys. Rev. Lett.* **105**, 057003 (2010).
[49] H. Sakakibara, H. Usui, K. Kuroki, R. Arita, and H. Aoki, *Phys. Rev. B* **85**, 064501 (2012).
[50] H. Sakakibara, K. Suzuki, H. Usui, K. Kuroki, R. Arita, D. J. Scalapino, and H. Aoki, *Phys. Rev. B* **86**, 134520 (2012).
[51] H. Sakakibara, K. Suzuki, H. Usui, S. Miyao, I. Maruyama, K. Kusakabe, R. Arita, H. Aoki, and K. Kuroki, *Phys. Rev. B* **89**, 224505 (2014).
[52] For a review on mixed-anion compounds, see, H. Kageyama, K. Hayashi, K. Maeda, J.P. Attfield, Z. Hiroi, J.M. Rondinelli, and K.R. Poeppelmeier, *Nat. Comm.* **9**,

- 772 (2018).
- [53] M. Hirayama, T. Tadano, Y. Nomura, and R. Arita, Phys. Rev. B **101**, 075107 (2020).
- [54] D. Li, K. Lee, B. Y. Wang, M. Osada, S. Crossley, H. R. Lee, Y. Cui, Y. Hikita, and H. Y. Hwang, Nature **572**, 624 (2019).
- [55] One of the reasons we consider these structures is because they are well known in cuprates. Further estimation of their stability as nickelates is left for future study.
- [56] J. P. Perdew, K. Burke, and M. Ernzerhof, Phys. Rev. Lett. **77**, 3865 (1996).
- [57] G. Kresse and D. Joubert, Phys. Rev. B **59**, 1758 (1999).
- [58] G. Kresse and J. Hafner, Phys. Rev. B **47**, 558(R) (1993).
- [59] G. Kresse and J. Hafner, Phys. Rev. B **49**, 14251 (1994).
- [60] G. Kresse and J. Furthmller, Comput. Mater. Sci. **6**, 15 (1996).
- [61] G. Kresse and J. Furthmller, Phys. Rev. B **54**, 11169 (1996).
- [62] P. Blaha, K. Schwarz, G. K. H. Madsen, D. Kvasnicka, and J. Luitz, WIEN2k, An Augmented Plane Wave + Local Orbitals Program for Calculating Crystal Properties (Karlheinz Schwarz, Techn. Universitt Wien, Austria, 2001).
- [63] N. Marzari and D. Vanderbilt, Phys. Rev. B **56**, 12847 (1997).
- [64] I. Souza, N. Marzari, and D. Vanderbilt, Phys. Rev. B **65**, 035109 (2001).
- [65] J. Kunes, R. Arita, P. Wissgott, A. Toschi, H. Ikeda, and K. Held, Comput. Phys. Commun. **181**, 1888 (2010).
- [66] A. A. Mostofi, J. R. Yates, Y.-S. Lee, I. Souza, D. Vanderbilt, and N. Marzari, Comput. Phys. Commun. **178**, 685 (2008).
- [67] N. E. Bickers, D.J. Scalapino, and S.R. White, Phys. Rev. Lett. **62**, 961(1989).
- [68] T. Tsujimoto, C.I. Sathish, Y. Matsushita, K. Yamaura, and T. Uchikoshi, Chem. Commun. **50** 5915 (2014).
- [69] V.I. Anisimov, D. Bukhalov, and T.M. Rice, Phys. Rev. B **59**, 7901 (1999).
- [70] H. Sakakibara, K. Suzuki, H. Usui, T. Kotani, H. Aoki, and K. Kuroki, arXiv: 1909.00060.
- [71] Y. Nomura, T. Nomoto, M. Hirayama and R. Arita, arXiv:2006.16943.
- [72] The five orbital model of La_2NiO_4 exhibits interorbital pairing as in Ref.[12] of $\text{Ba}_2\text{CuO}_{3+\delta}$. See the supplemental material for details.
- [73] Y. Nomura, M. Hirayama, T. Tadano, Y. Yoshimoto, K. Nakamura, and R. Arita, Phys. Rev. B **100**, 205138 (2019).
- [74] M. Kitatani, L. Si, O. Janson, R. Arita, Z. Zhong, and K. Held, arXiv:2002.1223.
- [75] X. Wu, D.D. Sante, T. Schwemmer, W. Hanke, H.Y. Hwang, S. Raghu, and R. Thomale, Phys. Rev. B **101**, 0605044(R) (2020).
- [76] L. Si, W. Xiao, J. Kaufmann, J.M. Tomczak, Y. Lu, Z. Zhong, and K. Held, Phys. Rev. Lett. **124**, 166402 (2020).
- [77] It is also interesting to note that the absence of superconductivity was reported in X.-R. Zhou, Z.-X. Feng, P.-X. Qin, H. Yan, S. Hu, H.-X. Guo, X.-N. Wang, H.-J. Wu, X. Zhang, H.-Yu Chen, X.-P. Qiu, Z.-Q. Liu, Rare Met. **39**, 368 (2020), where CaH_2 was not used to synthesize $(\text{Nd},\text{Sr})\text{NiO}_2$.
- [78] Q. Gu, Y. Li, S. Wan, H. Li, W. Guo, H. Yang, Q. Li, X. Zhu, X. Pan, Y. Nie, and H.-H. Wen, arXiv:2006.13123.
- [79] P. Adhikary, S. Bandyopadhyay, Tanmoy Das, Indra Dasgupta, and T. Saha-Dasgupta, arXiv:2005.01243.
- [80] Also during the finalization of our paper, Z. Wang, G.-M. Zhang, Y.-F. Yang, and F.C.Zhang, arXiv: 2006.15928 reported a theoretical study which adopts a different pairing mechanism, but attributes the difference in the pairing symmetry to the difference in the hole concentration.

Supplemental material: Designing nickelate superconductors with d^8 configuration exploiting mixed-anion strategy

Naoya Kitamine,¹ Masayuki Ochi,¹ and Kazuhiko Kuroki¹

¹Department of Physics, Osaka University, 1-1 Machikaneyama-cho, Toyonaka, Osaka, 560-0043, Japan

(Dated: July 3, 2020)

LATTICE CONSTANTS AND BAND STRUCTURES

In Fig.S1 and Figs.S2-S5, we plot the lattice constants obtained by structural optimization and the band structures, respectively, for all the materials considered in the present study. The lattice constants are larger for AE and/or X with larger ionic radius, except for the case of H in the T structure. As for the band structures, the relative position between the bands reflects the tendency seen in the on-site energy of each orbital (Fig.3 of the main text).

DEPENDENCE ON THE INTERACTIONS

Here, we vary the interaction values in the five orbital model of $\text{Ca}_2\text{NiO}_2\text{Cl}_2$ in various manners and see how the eigenvalue of the Eliashberg equation is affected. In Fig.S6(a), the interactions are varied maintaining $U' = U - 2J$ so as to satisfy orbital-rotation symmetry. Within the varied parameter range, larger U results in a suppression (slight enhancement) of superconductivity for $n < 4.2$ ($n > 4.2$). From Fig.S6 (b)

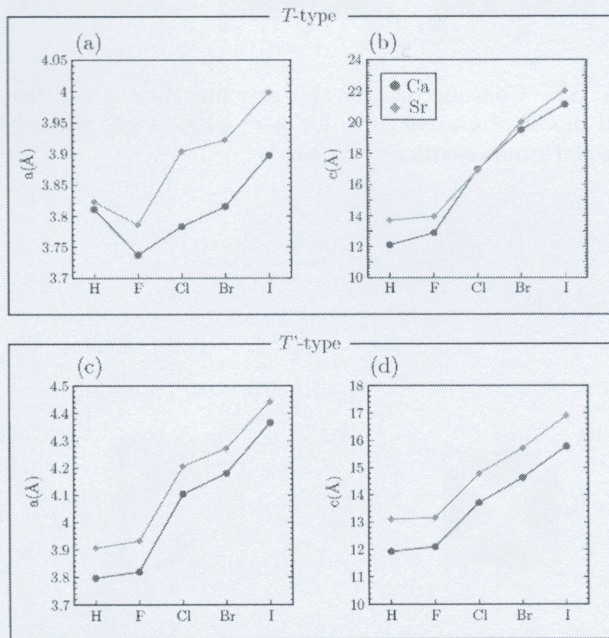


FIG. S1. Lattice constants for all the materials considered.

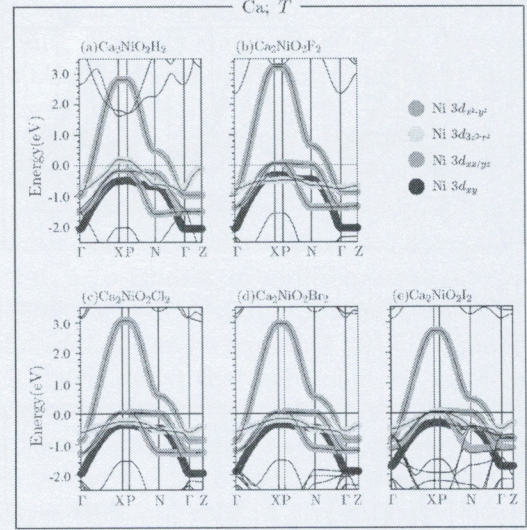


FIG. S2. Band structures of materials with $AE=\text{Ca}$ and the T structure. The band dispersion of the five orbital model is superposed to the first principles bands.

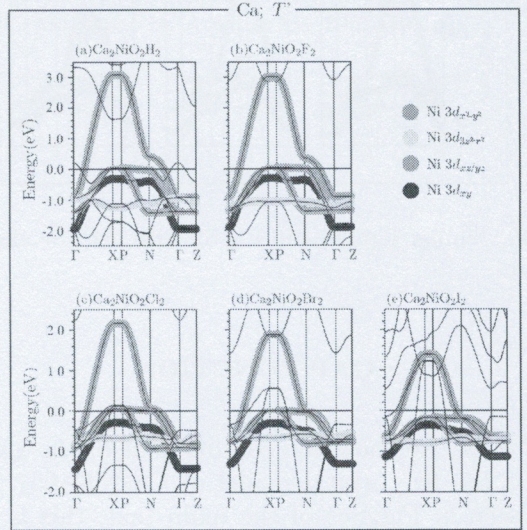


FIG. S3. Similar figure as in Fig.S2 with $AE=\text{Ca}$ and the T' structure.

to (d), one of U , U' , J , J' is varied, while others are fixed. The overall tendency is that increasing U' and J' enhances superconductivity, while increasing U and J degrades it.

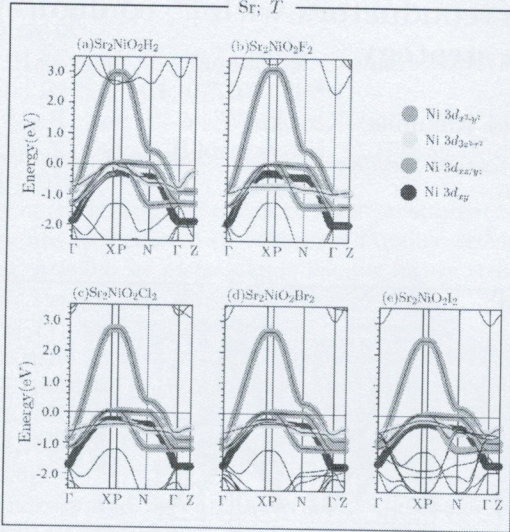


FIG. S4. Similar figure as in Fig.S2 with $AE=\text{Sr}$ and the T structure.

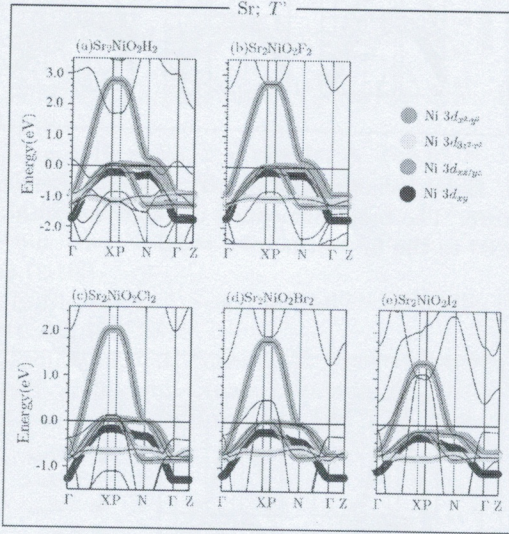


FIG. S5. Similar figure as in Fig.S2 with $AE=\text{Sr}$ and the T' structure.

GAP FUNCTION

In Fig.S7, we show the contour plot of the gap function for the five orbital model of $\text{Ca}_2\text{NiO}_2\text{Cl}_2$. As already seen in Fig.4(c) of the main text, this is an $s\pm$ -wave pairing with small k dependence of the gap, where the gap changes sign between the $d_{x^2-y^2}$ and incipient d orbitals. For La_2NiO_4 , there is no chance for superconductivity since λ is small, and, in the first place, we assume an unrealistic low-spin state. Nonetheless, we plot the inter-orbital and intra-orbital components of the gap function in Fig.S8. It is mainly intra-orbital $d_{x^2-y^2}$ -wave within the $d_{x^2-y^2}$ orbital, but there is also appreciable inter-orbital component between $d_{x^2-y^2}$ and $d_{3z^2-r^2}$ orbitals. This is similar to the case of $\text{Ba}_2\text{CuO}_{3+\delta}$ studied

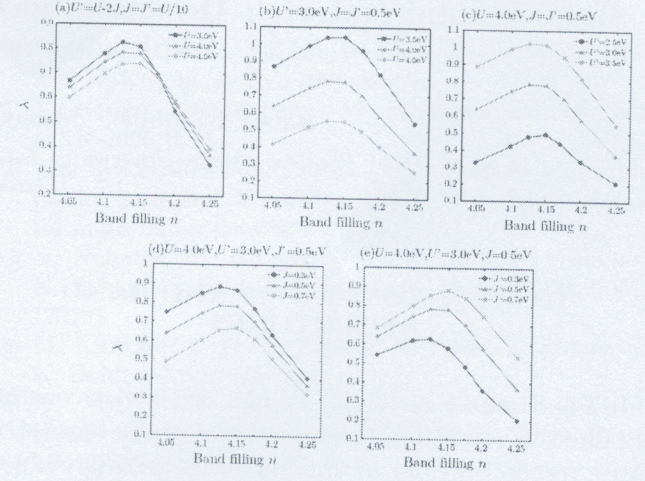


FIG. S6. Eigenvalue of the Eliashberg equation λ is plotted against the band filling n for various sets of interaction parameters. In (a), the interactions are varied maintaining $U' = U - 2J$ so as to satisfy the orbital rotational symmetry. From (b) to (d), one of U , U' , J , J' is varied, while the others are fixed.

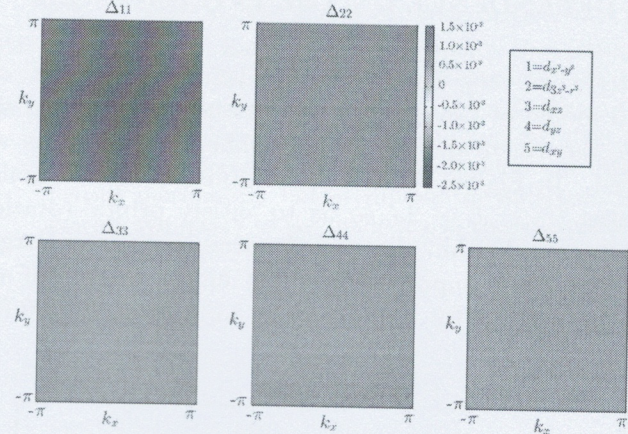


FIG. S7. Contour plot of the gap function of the five orbital model of $\text{Ca}_2\text{NiO}_2\text{Cl}_2$ for $n = 4.125$. Only the orbital-diagonal components are shown.

in Ref.[S1].

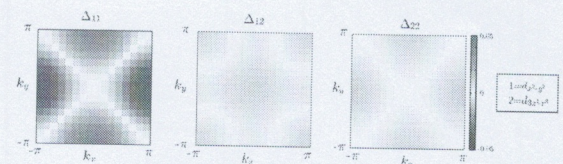


FIG. S8. Contour plot of the gap function of the five orbital model of La_2NiO_4 for $n = 4.125$. Here, we plot the off-diagonal component since it has appreciable amplitude.

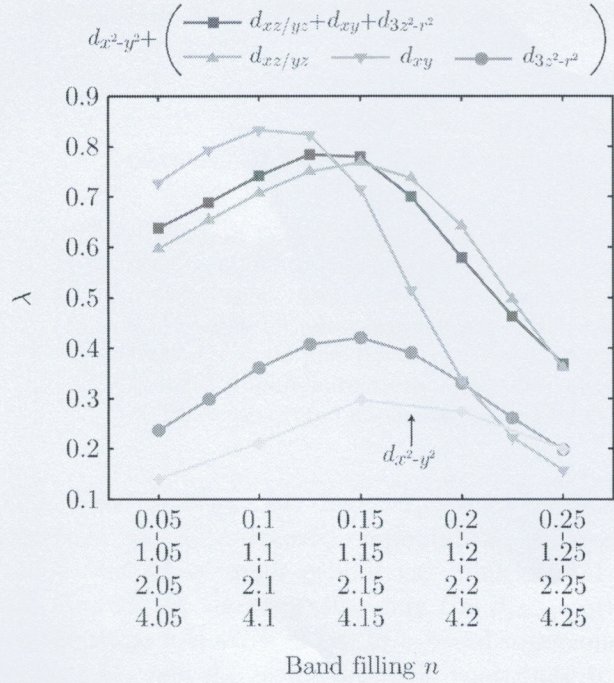


FIG. S9. λ against the band filling for various models of $\text{Ca}_2\text{NiO}_2\text{Cl}_2$.

ORBITAL DECOMPOSITION

In Fig.4(d) of the main text, we have only considered models that contain the $d_{xz/yz}$ orbitals (except for the single orbital model). The reason for this is as follows.

Since the top of the $d_{xz/yz}$ bands has the highest energy among the bands other than $d_{x^2-y^2}$ and the Fermi level for the stoichiometric band filling of $n = 4$ intersects only the $d_{x^2-y^2}$ and $d_{xz/yz}$ bands, the Fermi level of the full five orbital model with the band filling of $n (\geq 4)$ is the same as that of an n_{orb} orbital model with the band filling of $n - (5 - n_{\text{orb}})$, as far as the models that contain the $d_{xz/yz}$ orbitals are concerned. Conversely, the Fermi level of, say, a two-orbital $d_{x^2-y^2} + d_{xy}$ model with the band filling of $n - 3$ is not the same as that of the full five orbital model with the band filling of n . Hence, such models were not considered in the main text. Nonetheless, it is interesting to study how each band would affect superconductivity if other bands were absent. In Fig.S9, we plot the eigenvalue of the Eliashberg equation against the band filing for two-orbital $d_{x^2-y^2} + d_{xy}$ and $d_{x^2-y^2} + d_{3z^2-r^2}$ models, in addition to the $d_{x^2-y^2} + d_{xz/yz}$ model, the single orbital $d_{x^2-y^2}$ model, and the full five orbital model. It can be seen that all of the bands can act as an incipient band that enhances $s\pm$ superconductivity compared to the single orbital case. A tendency here is that the orbitals having larger $|\Delta E|$ (level offset with respect to the $d_{x^2-y^2}$ orbital, corresponding to $2t_{\perp}$ in the bilayer Hubbard model) give stronger enhancement of superconductivity, and superconductivity is optimized at lower band fillings.

[S1] K. Yamazaki, M. Ochi, D. Ogura, K. Kuroki, H. Eisaki, S. Uchida, and H. Aoki, arXiv:2003.04015.